Electron Holography of Field-Emitting Carbon Nanotubes

John Cumings and A. Zettl*
Department of Physics, University of California at Berkeley, Berkeley, California 94720
and Materials Sciences Division, Lawrence Berkeley National Laboratory, Berkeley, California 94720

M. R. McCartney[1] and J. C. H. Spence[2]
[1]*Center for Solid State Science, Arizona State University, Tempe, Arizona 85287-1504*
[2]*Department of Physics and Astronomy, Arizona State University, Tempe, Arizona 85287-1504*
(Received 18 April 2001; published 18 January 2002)

Electron holography performed *in situ* inside a high resolution transmission electron microscope has been used to determine the magnitude and spatial distribution of the electric field surrounding individual field-emitting carbon nanotubes. The electric field (and hence the associated field emission current) is concentrated precisely at the tips of the nanotubes and not at other nanotube defects such as sidewall imperfections. The electric field magnitude and distribution are stable in time, even in cases where the nanotube field emission current exhibits extensive temporal fluctuations.

DOI: 10.1103/PhysRevLett.88.056804 PACS numbers: 73.22.–f, 61.14.Nm

Electron holography is an electron interferometry technique that was developed primarily to increase the resolution of standard electron microscopy [1–3]. In addition, it can also give information about electromagnetic fields and has been used to measure the inner potentials of materials, contact potentials between materials, the Aharanov-Bohm effect, and magnetostatic and electrostatic fields in and around samples [4–9]. We here report the results of electron holography experiments performed on individual nanotubes subjected to external voltage bias including above the threshold for electron field emission. The experiments, performed *in situ* inside a transmission electron microscope (TEM), determine the phase and phase gradient of scattered TEM electrons from which the electric field distribution surrounding the charged nanotube is extracted. In our results, we find that the field strength is highest at the tips of the nanotubes and not at possible sidewall defects. We also find that the electric field distribution is highly stable even under conditions where the field emission current exhibits significant fluctuations.

Figure 1 shows a simplified schematic of our experimental setup. The experimental configuration merges the established technique of *in situ* TEM imaging of nanotubes under electron field emission conditions [10,11] with that of electron holography [12,13]. The upper portion of the figure shows a carbon nanotube independently voltage biased. Electrons field emitted from the nanotube are transferred predominantly horizontally and collected by a gold collector plate. Throughout the process the nanotube field emission current is carefully monitored. The vertical electron beam (shown) represents the TEM imaging beam. After traversing the nanotube region, this imaging electron beam is split by a fine-wire biprism. The two beam halves then converge and overlap onto a common imaging plane where the hologram is recorded. If the TEM electron source is quantum coherent, interference fringes will occur in the overlap region. The fringes contain information on the relative phase of the two beam halves and, in particular, give direct information about the local potentials traversed by the imaging beam around the nanotube.

To accurately position the nanotubes relative to the TEM column as well as to the gold collector plate a specially constructed piezodriven manipulation stage [10,11,14] was used inside the TEM (Phillips CM200 FEG, operated at 200 keV, utilizing a Lorentz lens) equipped with a rotatable Möllenstedt-type biprism [15]. Images were captured using a 1024 × 1024 CCD from Gatan, Inc. Multiwall carbon nanotubes grown by the conventional arc-plasma method [16] were mounted to the manipulation electrode using conducting epoxy. The nanotubes were typically positioned about 6 μm away from the gold electrode and a

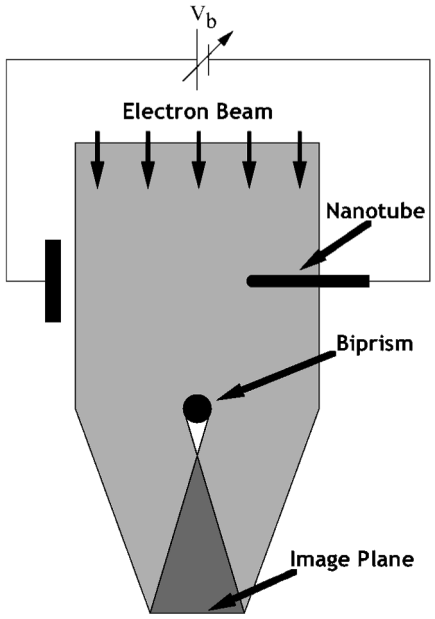

FIG. 1. Schematic diagram of the experimental setup used for nanotube holography measurements.

bias voltage, V_b, was applied between the two. Field emission current was monitored using a DL Instruments 1211. In a typical experiment, a quick holographic survey determines where the electric fields are the strongest during field emission, and holographic information is recorded for a protruding nanotube in this region for a series of bias voltages. For the experiments reported here nanotube electron field emission was first significant at a bias of $V_b = 70$ V (with a field emission current of 40 pA). At $V_b = 120$ V the total field emission current was 0.54 μA. Similar results to those presented here have been obtained for a number of nanotube samples.

Figure 2 shows a hologram of a nanotube with applied bias $V_b = 120$ V, well above the threshold voltage for electron field emission for this nanotube. The large dominant fringes visible in Fig. 2A are Fresnel fringes caused by the presence of the biprism in the imaging beam path and do not carry any information about the electric fields surrounding the nanotube. Figure 2B shows an enlarged view of the boxed region of the hologram in Fig. 2A. In Fig. 2B there are apparent small-scale interference fringes (with a periodicity of roughly 4 nm). It is these small-scale hologram fringes that carry detailed information about the electric field distributions in the region of the nanotube. The size of the fringes also determines the spatial resolution of the holography. The amplitude of the fringes is approximately 2% of the total intensity, which is sufficient to accurately measure the phase.

In order to extract the desired nanotube electric fields, two stages of hologram analysis are necessary. In the first analysis stage, a Fourier transform method [12] is used to determine the phase shift and phase gradient relevant to the interference fringes. In the second analysis stage, the phase shift and phase gradient are used to determine quantitatively the electric potential distributions in and around the nanotube. The phase shift ($\Delta\phi$) that an electron acquires traversing a spatially dependent potential V is given by

$$\Delta\phi = \alpha \int_{\text{beam path}} V\, dl\,, \qquad (1)$$

where α is a parameter that depends on the accelerating voltage of the electron microscope. For the present experiments performed with a 200 keV TEM imaging beam, α is 7.29 mrad per V-nm. The phase reconstruction calculations were done using the Digital Micrograph software package (Gatan, Inc.).

Figure 3 shows in the left-hand column a series of phase shift maps obtained by Fourier transform analysis of hologram images recorded at selected nanotube bias V_b, both below and above the threshold for nanotube electron field emission. The upper phase shift map is for $V_b = 0$ V, and here the featureless area around the nanotube demonstrates that, in the region surrounding the nanotube, the imaging electron beam has a uniform phase. In this phase shift map the nanotube itself appears; the portion of the imaging beam that "goes through" the nanotube is shifted

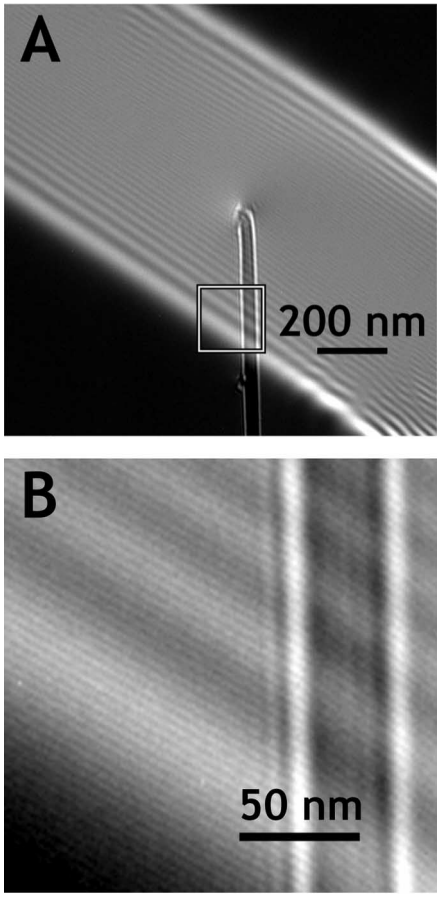

FIG. 2. (A) An electron hologram of a carbon nanotube biased at 120 V in the field-emission regime. (B) An enlarged view of the boxed region in (A), clearly showing the fine interference structure of the hologram.

by a uniform 3.1 rad from the background phase. This contrast is due to the difference in the integrated potential [Eq. (1)] for the imaging beam inside the nanotube relative to the vacuum potential [12]. From these zero-bias data, we find a mean "inside" potential for the nanotube of 12 V, in agreement with previous measurements on other carbon materials [12,13,17]. The center and lower phase shift maps in the left-hand column of Fig. 3 are calculated from holograms taken at $V_b = 70$ V and $V_b = 120$ V, just above and significantly above the threshold bias for field emission for this nanotube. In these phase shift maps the phase shift due to the applied nanotube bias is strikingly apparent. In these modulo-2π plots, whenever the phase shifts by 2π it wraps back to zero, causing stripes in the phase map. These stripes show the equiphase contour lines of the original hologram.

The right-hand column of images in Fig. 3 represents phase gradient data associated with the phase shift maps just discussed. These maps are determined by calculating the magnitude of the two-dimensional gradient directly from the phase shift maps shown to the left. For $V_b = 0$ V, the phase gradient is featureless in the region surrounding the nanotube, while for $V_b = 70$ and 120 V (in the field emission region), the phase gradient is clearly

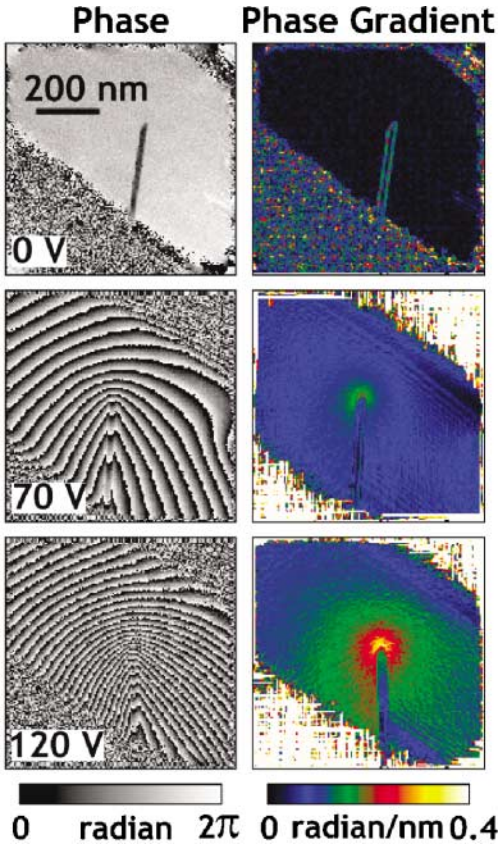

FIG. 3 (color). Phase shift and phase gradient maps extracted from holograms of the same nanotube at bias voltages $V_b = 0$, 70, and 120 V. The phase gradient indicates where the electric field is the strongest; note the concentration of the electric field at the nanotube tip for $V_b = 70$ and 120 V.

concentrated at the tip of the nanotube. It is tempting to associate the phase and phase gradient maps of Fig. 3 with the physical electric potential and electric field distributions, respectively. With appropriate caveats (discussed below), this analogy is in fact meaningful. The phase shift maps in the left-hand column of Fig. 3 qualitatively represent electric potential maps, and the equiphase lines are fair representations of the equipotential lines in the region around the nanotube. Within the nanotube and along its length, however, the phase shift maps of Fig. 3 show, for $V_b = 70$ and 120 V, a series of phase shift 2π rollovers. As we discuss below, these rollovers within the nanotube do not in themselves imply that the physical voltage is dropping along the length of the nanotube. Additionally, the phase gradient maps of Fig. 3 are a fair qualitative representation of the electric field strength external to the nanotube. Most importantly, the high phase gradient at the tip of the nanotube for $V_b = 70$ and 120 V demonstrates that the electric field is most intense at the tip of the nanotube. Even for large nanotube bias voltages, we see no evidence for high concentrations of electric field at other locations along the nanotube length. Since the local electric field dictates electron field emission, these results imply that nanotube electron field emission occurs at the tips of nanotubes and that sidewall defects or other field-concentrating geometric or electronic irregularities are not required for field emission.

We now turn to the quantitative determination of the three-dimensional electric field distributions within and surrounding the nanotube. This difficult problem is solved most directly by iteratively creating a model potential (derived from a model charge distribution), which, from Eq. (1), ultimately yields the correct (experimentally determined) phase shift map. Our starting model [18] is a one-dimensional line of charge, with a complementary image charge distribution (due to the induced charges on the gold collector plate). We then allowed the linear charge density to be a variable function of position along the nanotube axis. We varied the linear charge density until the model produced a cylindrical equipotential surface of fixed radius capped by a hemisphere of the same radius, with the potential constant to within 0.1%.

The phase shift and phase gradient maps determined from the model nanotube potential are shown in Fig. 4; they match closely the data for the field emitting nanotube biased at $V_b = 120$ V. The fit yields an electric field strength at the tip of the nanotube $E = 1.22$ V/nm. Electric field strengths at the nanotube tip were similarly determined for $V_b = 90$ V and $V_b = 70$ V and are 0.82 V/nm and 0.64 V/nm, respectively. These field strengths are consistent with field emission, indicating that no other field sources, such as sidewall defects, are required to account for the nanotube field emission. Measurements on different nanotubes showed that, for the same applied bias voltage, the local electric field at the tip of the nanotube is inversely proportional to the nanotube radius. It is important to note that the nanotube in the model has a constant potential along its length, yet the equiphase lines cut through the nanotube, just as they do in the experimental data of Fig. 3. This is simply a result of increased path length in the integral of Eq. (1). Therefore, the holography is consistent with no potential drop along the length of the nanotube, even in the strongly field-emitting regime [19].

We now turn our attention to fluctuations in the field emission current and their possible origin. In the field emission regimes here investigated, the nanotube emission current was observed to fluctuate greatly over the course of observation similar to experiments reported elsewhere [20–22]. In some cases, the current varied by as much as 80% of its peak value over a time period of hundreds of milliseconds. The fluctuations, however, can not be attributed to the field distributions we measure in the vicinity of the nanotube. If the phase shift varies during the exposure time of a hologram, then the fringes in a hologram can become blurred, and if the fluctuations cause phase shifts on the order of π, then the fringes will disappear altogether. From our model of the nanotube phase, we estimate that a fluctuation of only 0.03 V/nm in the strength of the electric field at the tip of the nanotube could cause the fringes to be completely blurred. For the current work, 4 s exposure times were used to capture the holograms, which

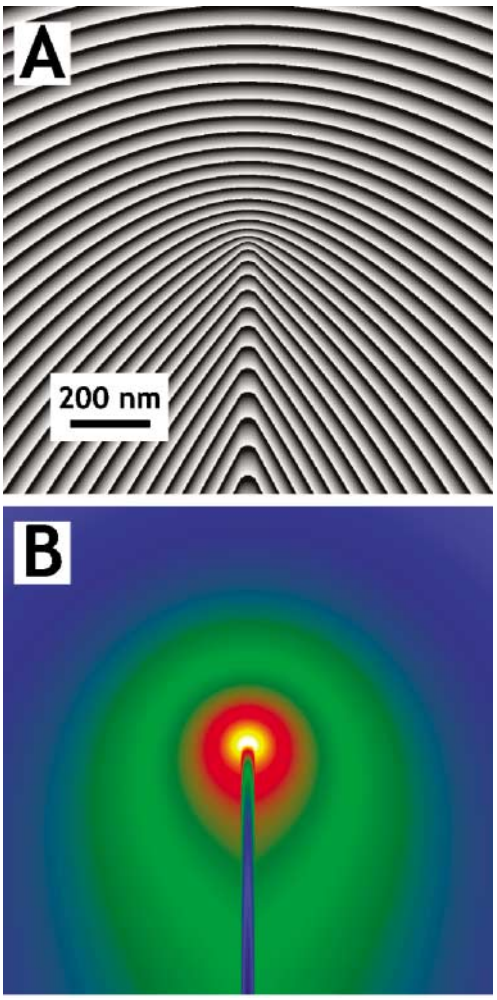

FIG. 4 (color). Model phase shift (A) and phase gradient (B) for a nanotube with $V_b = 120$ V.

is much longer than the time period of the fluctuations in the emission current. We therefore conclude that the magnitude of the electric field distribution varied by less than 2.5% during the exposure of the hologram. In addition, we have repeatedly recorded holograms on the same tube, with successive measurements separated by several minutes, and find that the differences in the extracted electric field strengths are at most 7%, which is within the estimated error of the technique.

We conclude that the origin of nanotube field emission current fluctuations cannot be a mechanism tied to changes in the overall electric field magnitude or distribution. For example, unraveling of the nanotube fabric at the tip, or strong fluctuating intertube interactions suggested previously [20,22], appear unlikely mechanisms. It is more likely that subtle changes in the tip electronic structure, as might occur with tip adsorbates [23], alter the emission current without significant changes in the overall electric field distribution.

We acknowledge the use of facilities in the Center for High Resolution Electron Microscopy at Arizona State University. J. C. and A. Z. acknowledge support by DOE Grant No. DE-AC03-76SF00098 and by NSF Grants No. DMR-9801738 and No. DMR-9501156. J. C. H. S. acknowledges support by NSF Grant No. DMR-9814055.

*Corresponding author.

[1] D. Gabor, Nature (London) **161**, 777 (1948).
[2] L. Marton, Phys. Rev. **85**, 1057 (1952).
[3] A. Orchowski, W. D. Rau, and H. Lichte, Phys. Rev. Lett. **74**, 399 (1995).
[4] G. Möllenstedt and M. Keller, Z. Phys. **148**, 34 (1957).
[5] E. Krimmel, W. Rothemund, and G. Möllenstedt, Appl. Phys. Lett. **5**, 209 (1964).
[6] Y. Aharanov and D. Bohm, Phys. Rev. **115**, 485 (1959).
[7] T. Matsuda *et al.,* Phys. Rev. Lett. **62**, 2519 (1989).
[8] J. W. Chen *et al.,* Phys. Rev. A **40**, 3136 (1989).
[9] For a review of applications, see A. Tonomura, Rev. Mod. Phys. **59**, 639 (1987).
[10] Z. L. Wang, P. Poncharal, and W. A. de Heer, J. Phys. Chem. Solids **61**, 1025 (2000).
[11] Z. L. Wang, P. Poncharal, and W. A. de Heer, Microsc. Microanal. **6**, 224 (2000).
[12] E. Völkl, L. F. Allard, and D. C. Joy, *Introduction to Electron Holography* (Kluwer/Plenum, New York, 1999).
[13] A. Tonomura, *Electron Holography* (Springer, Berlin, New York, 1999).
[14] W. K. Lo and J. C. H. Spence, Ultramicroscopy **48**, 433 (1993).
[15] G. Möllenstedt and H. Düker, Naturwissenschaften **42**, 41 (1955).
[16] T. W. Ebbesen and P. M. Ajayan, Nature (London) **358**, 220 (1992).
[17] X. Lin and V. P. Dravid, Appl. Phys. Lett. **69**, 1014 (1996).
[18] G. Matteucci, G. F. Missiroli, M. Muccini, and G. Pozzi, Ultramicroscopy **45**, 77 (1992).
[19] The phase extracted from the holograms is the phase difference between the imaging beam which passes through the sample and the reference beam which does not pass through the sample. If the reference passes through a potential, it can also acquire phase information. The reference crosses the specimen plane approximately 2 μm away from the nanotube. At this distance, the fringing field due to the nanotube does not add significantly to the fit of the model. Fields from other sources will introduce a small error of 10%. We have also examined phase shifts due to magnetic fields induced by the field emission current; this contribution is insignificant.
[20] A. G. Rinzler *et al.,* Science **269**, 1550 (1995).
[21] P. G. Collins and A. Zettl, Appl. Phys. Lett. **69**, 1969 (1996).
[22] P. G. Collins and A. Zettl, Phys. Rev. B **55**, 9391 (1997).
[23] K. A. Dean and B. R. Chalamala, Appl. Phys. Lett. **76**, 375 (2000).